Accepted Manuscript

A chemiluminescence biosensor for the detection of thrombin based on the aptamer composites

Yanna Lin, Jianbo Li, Yanhui Wang, Yuanling Sun, Chaofan Ding, Weiyan Sun, Chuannan Luo

PII:	S1386-1425(17)30881-8
DOI:	doi:10.1016/j.saa.2017.10.074
Reference:	SAA 15580
To appear in:	*Spectrochimica Acta Part A: Molecular and Biomolecular Spectroscopy*
Received date:	25 May 2017
Revised date:	4 August 2017
Accepted date:	27 October 2017

Please cite this article as: Yanna Lin, Jianbo Li, Yanhui Wang, Yuanling Sun, Chaofan Ding, Weiyan Sun, Chuannan Luo , A chemiluminescence biosensor for the detection of thrombin based on the aptamer composites. The address for the corresponding author was captured as affiliation for all authors. Please check if appropriate. Saa(2017), doi:10.1016/j.saa.2017.10.074

A chemiluminescence biosensor for the detection of thrombin based on the aptamer composites

Yanna Lin, Jianbo Li, Yanhui Wang, Yuanling Sun, Chaofan Ding, Weiyan Sun, Chuannan Luo*

Key Laboratory of Interfacial Reaction & Sensing Analysis in Universities of Shandong, School of Chemistry and Chemical Engineering, University of Jinan, Jinan 250022, PR China

Corresponding author: Tel.: +86 0531 89736065. E-mail address: chm_sunyl@126.com

Abstract

An efficient, rapid, simple and ultrasensitive chemiluminescence (CL) approach was proposed for thrombin detection based on the aptamer-thrombin recognition. The aptamer composites were synthesized in this work using graphene oxide (GO) as the backing material. The thrombin was adsorbed on the aptamer composites based on the aptamer-thrombin recognition. Thus, thrombin could be quantified by the difference value of the CL intensity between supernate of the sample and the mixture which composed of thrombin and coexisted substances. The CL intensity exhibits a stable response to thrombin over a concentration range from 2.5×10^{-10} to 1×10^{-9} mol • L^{-1} with a detection limit as low as 8.3×10^{-11} mol • L^{-1}, the relative standard deviation (RSD) was found to be 4.9% for 11 determinations of 1.25×10^{-9} mol • L^{-1} thrombin. Finally, the applicability of the method was verified by applying to serum samples. The recoveries were in the range of 90.3-101.0% with RSD of 2.6-3.2%.

Keywords: Aptamer; Thrombin; Flow injection chemiluminescence; Graphene oxide.

Introduction

Aptamers are a kind of DNA or RNA strands selected by the SELEX technology, which was set up in the 1990s originally. Aptamers have been applied to biosensing [1-4], therapeutics [5,6] and diagnostics [7,8]. Generally, aptamers can play the role similar to that of the antibodies in therapeutic applications [9]. Compared with antibodies, aptamers have some advantages, such as lower molecular weight, better stability, higher binding affinity and cheaper. As we know, G-rich DNA can form a G-quadruplex structure [10]. The structure can be stabilized when aptamers were bound to specific targets including organic molecules, protein and cell, et al. Thus, some electrochemistry [11-12], transistorsensor [13], chemiluminescence [14] and colorimetric [15] detection strategies for detection of targets based on G-quadruplex structure have been reported.

Graphene oxide (GO) is a derivative of graphene. It has a large specific surface area and many functional groups including epoxy group, carboxyl and hydroxide radical. Especially, the applications of GO-based materials have attracted much attention in the past few years [16-24]. In addition, the GO-based sensors [25] exhibit a number of convenient features for large-scale manufacturing such as transparency, flexibility and suitability.

Thrombin is a kind of serine protease, and plays an important role in molecular biology. Thrombin also is the main effective enzyme of blood coagulation cascade reaction and has a central role in the initiation and propagation of thrombotic diseases. Due to its biological importance, techniques including electrochemistry [26],

fluorescence [27], chemiluminescence [28], and surface-enhanced Raman spectroscopy [29] etc. have been applied to thrombin detection. For example, Zhang [30] constructed an electrochemiluminescence aptasensor and Li [31] developed a chemiluminescence aptasensor, all of which were used to the detection of thrombin. But in the former electrochemical method, the process of electrode modification is slow and time consuming while the latter chemiluminescence method with relatively low sensitivity - the detection limit of 1×10^{-9} mol·L^{-1}. Modern analytical chemistry emphasizes the "3S" principle, that is, sensitivity, specificity, speed. The flow injection chemiluminescence only requires simple instruments and operation, and has some advantages of speediness and ultrasensitivity. Therefore, it has been applied to a variety of analytical tests [32-34].

Aptamer composites containing magnetic nanoparticles were synthesized in this work. The aptamer composites exhibited excellent merits for higher selectivity, better stability, and easier separation, etc. The main reasons for higher selectivity and better stability are attributed to the aptamer composites and the G-quadruplex structure [35] which is formed by aptamer and thrombin. Thus, a novel CL sensor for thrombin was prepared, in which the dispose of samples was performed by aptamer composites with high selectivity, high absorbance and fast separation. Under the optimal conditions of CL, the aptamer composites were applied to the detection of thrombin in serum samples with high selectivity and sensitivity, successfully.

Experimental section

Chemicals and materials

Thrombin aptamer was synthesized by Sangon Biotechnology Co. Ltd. (Shanghai, China). The sequence of aptamer was 5'NH_2-ATAGGTTGGTGTGGTTGG-3'. Imidazole was supplied from Aladdin Bio-chem Technology Co; 1-(3-Dimethylaminopropyl)-3-ethylcarbodiimide (95%) and absolute ethanol (A.R) were purchased from Sinopharm Chemical Reagent Co. Ltd.. Ltd. The H_2O_2, $FeCl_3$, $FeCl_2$, $NH_3 \cdot H_2O$ and all other chemicals unless specified were of analytical reagent grade and used without further purification. Phosphate buffer solution (PBS) and redistilled water were used throughout the work.

Apparatus

The IFFM-E flow injection CL analyzer (Xi'an Remex Electronic instrument High-Tech Ltd., China) which consists of an automatic injection system and a detection system was used in this work. The schematic diagram of the CL sensor used in this work was shown in Fig. 1. In order to obtain a better stability, the instrument runs for at least 10 min before the first operation. The CL sensor was used to optimize the concentration of reagents and determine the thrombin in the samples.

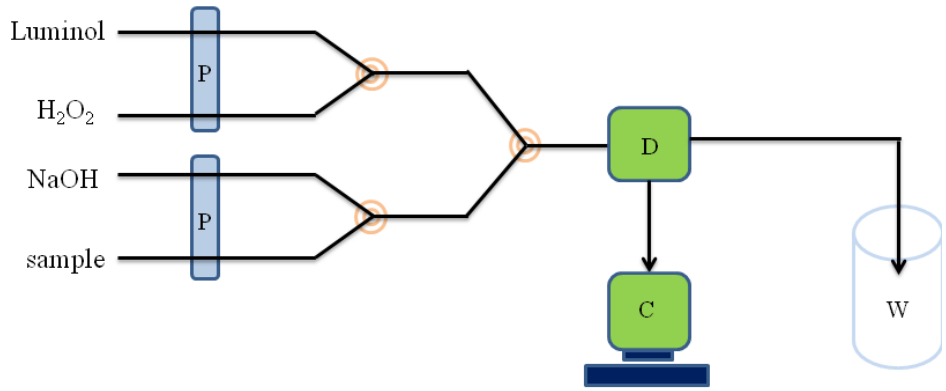

Fig. 1. The schematic diagram of the CL sensor. P: pump, C: computer, D: detector, W: waste.

Preparation of aptamer composites

The graphene oxide was synthesized by the modified method of Hummers [36]. First, 1.0 g of graphite powder and mixed acid were added into a 500 mL flask, and then cooled followed by stirring. The mixed acid was composed of H_2SO_4 and HNO_3 (V_{H2SO4}/V_{HNO3} 9:1). Then, 6.0 g of $KMnO_4$ was added gradually under stirring. The diluted suspension was stirred at 90 ºC, followed by addition of H_2O_2 (30%). Finally, the mixture was centrifugalized and washed with 0.2 mol • L^{-1} HCl solution, followed by water washing till the pH = 7.0. The GO was obtained as brown powder after dried at 60 ºC under vacuum.

Magnetic graphene oxide (MGO) was prepared according to the methods of Kassaee's group [37]. The magnetic composite was prepared by added 0.2 g of GO to double-distilled water, and the solution was ultrasonically dispersed into a homogeneous suspension. Subsequently, 0.2 g of $FeCl_3$ and 0.14 g of $FeCl_2$ were added to the GO suspension, and the value of pH was adjusted to 9.0 with NH_3 • H_2O under the protection of N_2. Finally, the diluted suspension was stirred at 90 ºC and refluxed for 0.5 h. The precipitate was isolated in the magnetic field. The obtained MGO was washed with 150 mL of absolute ethanol, and then the products were air-dried.

Aptamer composites were prepared according to the previous literature as reported [38]. The method was modified as follows:

Firstly, 0.05 g of MGO was dispersed in 100 mL of PBS, ultrasonic dispersion for 30 min. Subsequently, 0.043 g of imidazole, 140 μL of aptamer solution and 0.056 g of EDC were added into the suspension, respectively. Then, the aptamers were

incubated for 8 h at room temperature. Finally, the aptamer composites were isolated in the magnetic field. The products were stored in the 100 mL volumetric flask at 4 ^{o}C.

The collection of real sample

Bovine serum, super horse serum and goat serum were purchased from Sangon Biotechnology Co. Ltd. and used in this work. These serum samples were treated as follows:

Firstly, the serums were removed from the freezer and placed in a refrigerator at 4 ^{o}C for about 12 h. Next, the serum samples were regularly shook at room temperature to make it fully soluble. Then, the serum samples were centrifugated at 12000 rpm for 35 min and then the eluents were diluted with PBS buffer solution before measurements.

Results and discussions

The characterization of GO and MGO

The morphology and structure of all of the composites were studied by SEM, XRD and FTIR.

From the SEM image (Fig. 2A), the thickness of GO was fold of thin monolayer structure and the surface is rough, which increased the specific surface area, immensely. While on the surface of MGO (Fig. 2B), as seen, there were multi-layer. The surface was rugged and coated by Fe_3O_4.

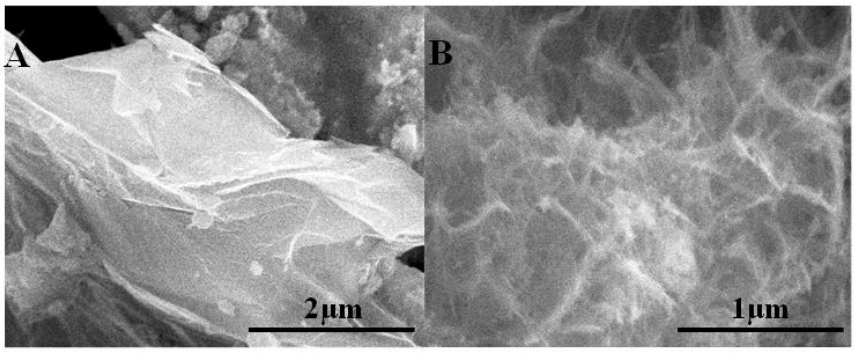

Fig. 2. The SEM of GO (A) and MGO (B)

In the XRD patterns (Fig. 3A), there was a narrow and relatively strong diffraction peak at about 2θ = 10º, that was the characteristic peak of GO. As seen, the diffraction peak at 2θ = 30.2º, 35.5º, 43.2º, 53.6º, 57.1º and 62.7º were the six characteristic peaks of Fe_3O_4, which demonstrated the MGO was synthesized successfully.

The chemical groups on the surface of GO and MGO were investigated by FTIR spectra, shown in Fig. 3(B). In the spectrum of GO, the absorption peaks at 1600 - 1400 cm^{-1} were the characteristics of benzene ring, the absorption peak at 1055 cm^{-1} indicated the C-O group's stretching vibration. As shown, the peak at 620 cm^{-1} was the characteristic of Fe_3O_4, which provided a solid support that MGO was synthesized successfully.

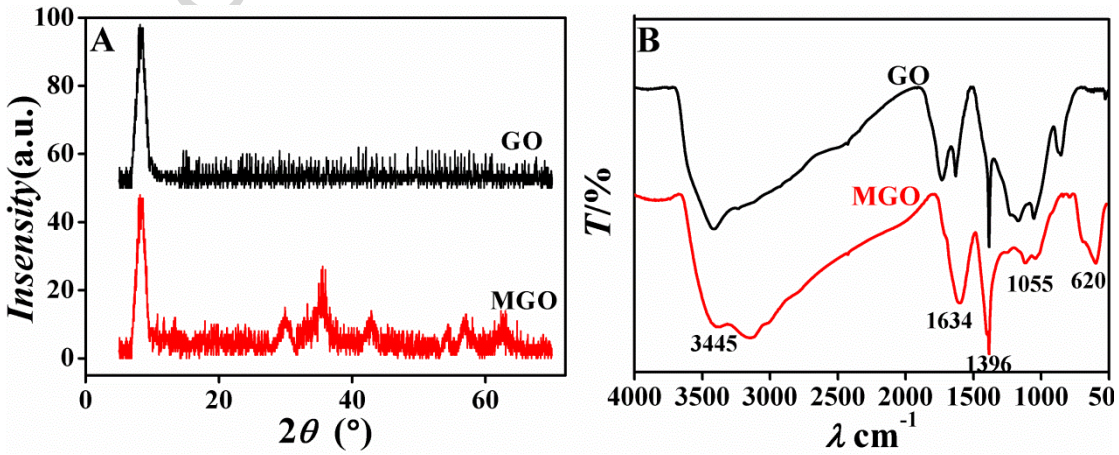

Fig. 3. The XRD patterns of GO and MGO (A); the FTIR of GO and MGO (B).

The possible mechanism of the CL seneor

In the chemiluminescence system, H_2O_2 can be instantly decomposed into HOO^- in alkaline medium (reaction (1)). Then, the resulting HOO^- continues to react with H_2O_2 to produce HOO• and HO• (reaction (2)). The HOO• and HO• could oxidize luminol to produce CL. Thrombin is composed of two chains that named A and B, respectively. In the structure of thrombin, the prominent loop around K70 is the outer binding site Ⅰ which contains positively charged amino acid residues (Lys 36, Lys 149E, Arg 73, Arg 77A), and there also is a positively charged amino acid residue region in the vicinity of the C-terminal α-helix of the B chain, the region is outer binding site Ⅱ [39, 40]. Therefore, we think the possible mechanism is that those two positively charged binding sites could combine with HOO^- by electrostatic interaction, which can lead to a decrease in the concentration of HOO• and HO• in the solution. Thus, the CL intensity decreased after the thrombin was added to the solution, as shown in Scheme 1., thrombin CL value $\Delta I = I_2 - I_1$. The experimental results are shown in the Fig. 4.

$$H_2O_2 + OH^- \rightarrow HOO^- + H_2O \quad (1)$$

$$HOO^- + H_2O_2 \rightarrow HOO\bullet + HO\bullet + OH^- \quad (2)$$

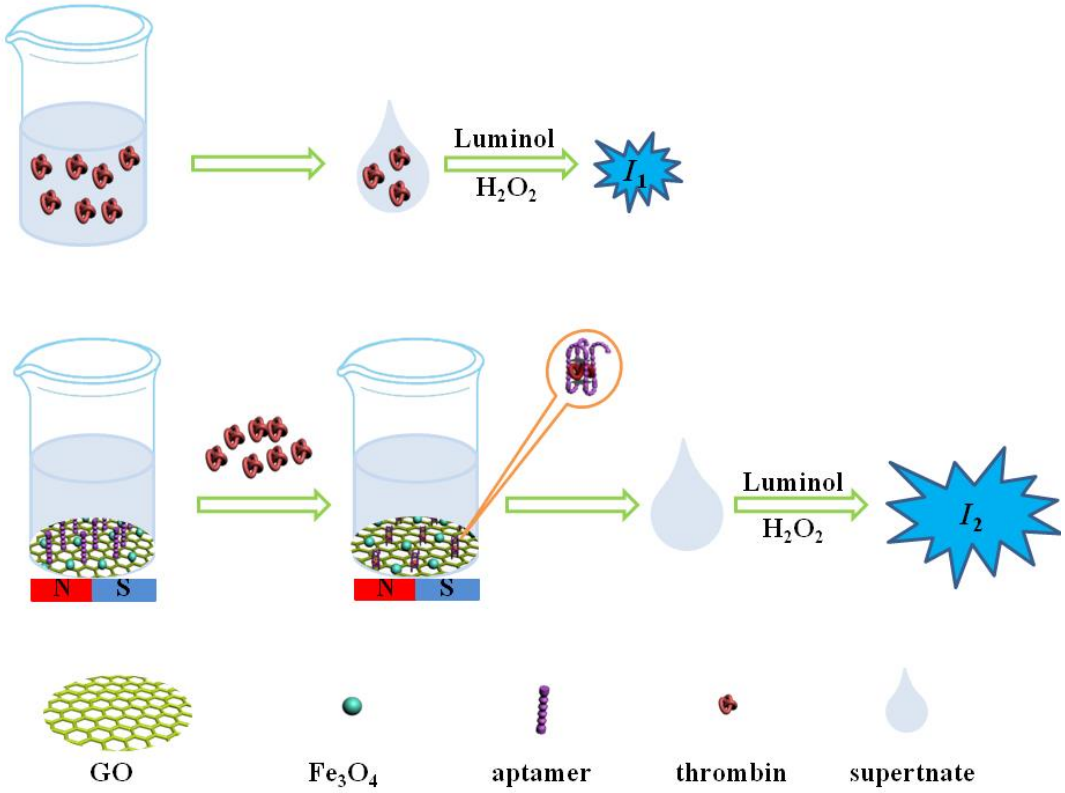

Scheme 1 Schematic illustration of the detection of thrombin based on CL sensor

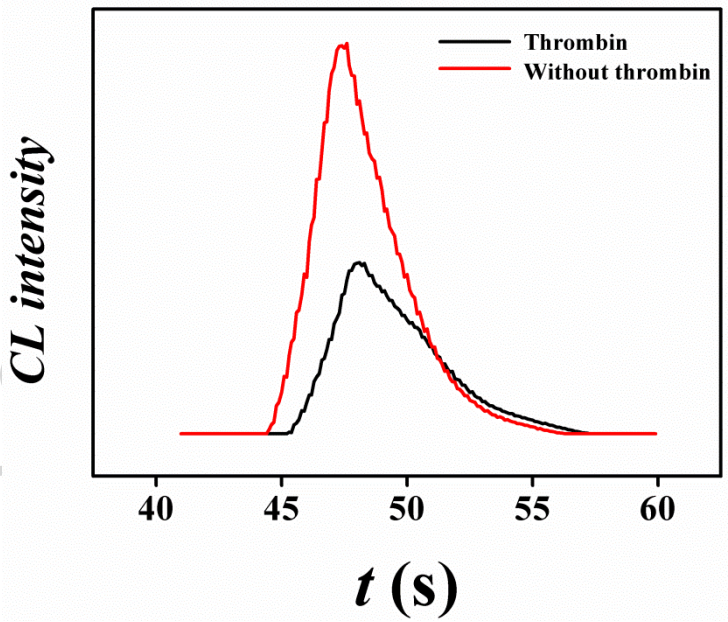

Fig. 4. CL intensity of thrombin and without thrombin. Experimental conditions: luminol, 1.25×10^{-4} mol • L^{-1}; H_2O_2, 0.01 mol • L^{-1}; NaOH, 0.01 mol • L^{-1}.

The optimization of CL reaction conditions

To achieve the high sensitivity of the assay, the reaction conditions were

optimized in this work. When the main pump speed was up to 30 r • min^{-1}, the CL signal reached the maximum. In addition, the CL intensity reached the maximum when vice pump speed was 35 r • min^{-1}. In order to select the optimal oxidant, luminol-H_2O_2, luminol-$KMnO_4$, luminol-$Ce(SO_4)_2$, luminol-$K_3[Fe(CN)_6]$, and luminol-KIO_4 CL systems were constructed, and the CL intensity of these CL systems were measured in alkaline medium in this work, as shown in Fig. 5. The color of the solution of $KMnO_4$, $Ce(SO_4)_2$ and $K_3[Fe(CN)_6]$ could interfere with CL, and KIO_4 is toxic. Therefore, H_2O_2 is the optimal oxidant in this work.

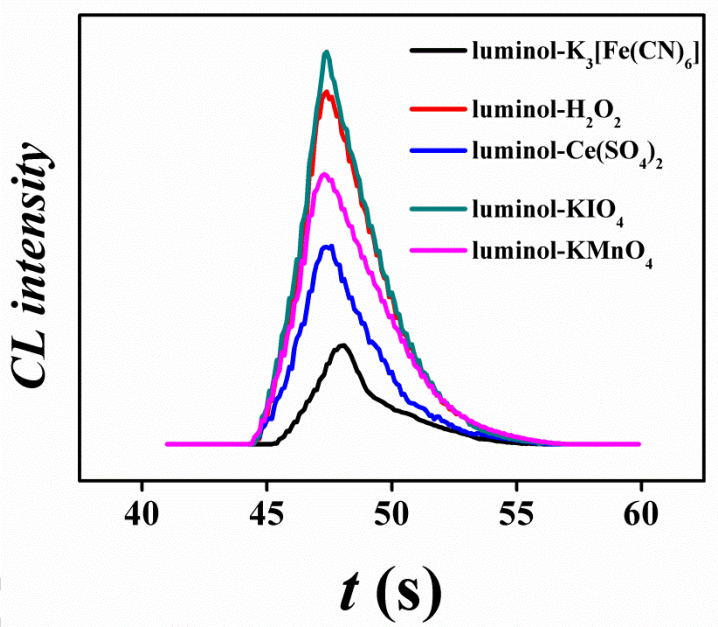

Fig. 5. CL intensity of luminol-H_2O_2, luminol-$KMnO_4$, luminol-$Ce(SO_4)_2$, luminol-$K_3[Fe(CN)_6]$, and luminol-KIO_4. Experimental conditions: luminol, 1.25×10^{-4} mol • L^{-1}; NaOH, 0.01 mol • L^{-1}; H_2O_2, $KMnO_4$, $Ce(SO_4)_2$, $K_3[Fe(CN)_6]$ and KIO_4, 0.01 mol • L^{-1}.

The reagents' optimization results were shown in Fig. 6. Only under the optimal conditions, could the CL intensity reach the maximum which was suitable for the detection of thrombin.

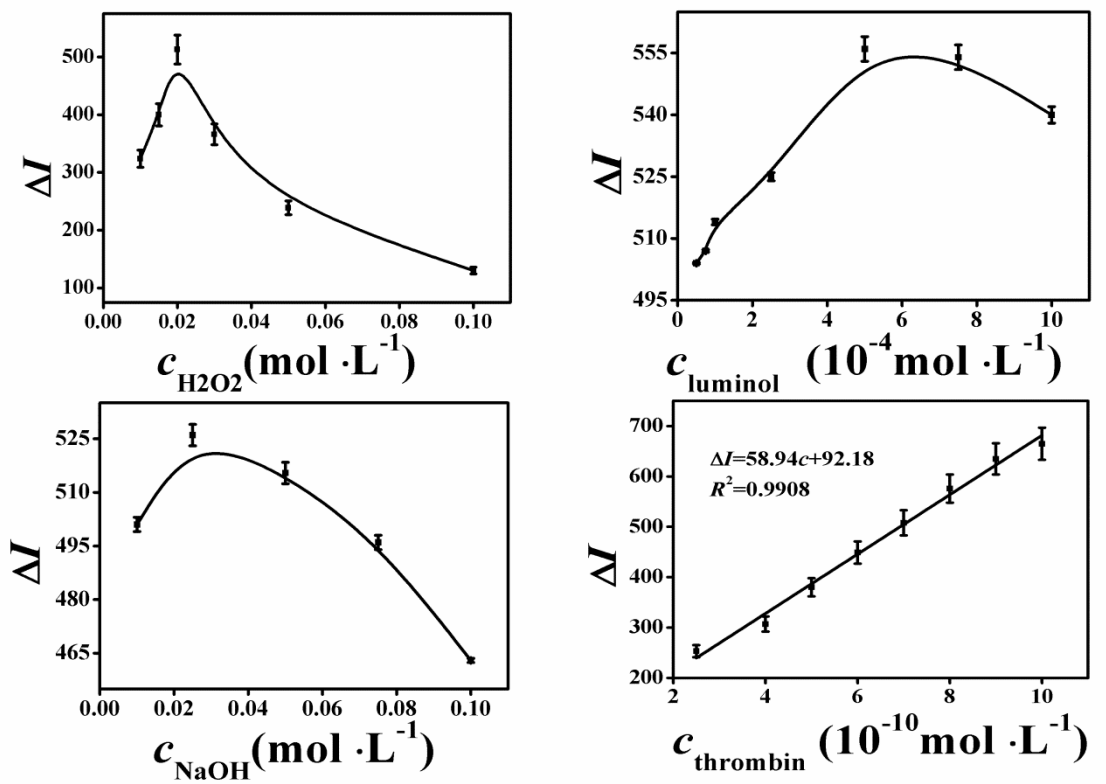

Fig. 6. The option of CL reaction conditions: (A) Effect of H_2O_2 concentration: luminol, 1.25×10^{-4} mol • L^{-1}; NaOH, 0.01 mol • L^{-1}; (B) the effect of luminol concentration: H_2O_2, 0.025 mol • L^{-1}; NaOH, 0.01 mol • L^{-1} and (C) the effect of NaOH concentration: luminol, 5×10^{-4} mol • L^{-1}; H_2O_2, 0.025 mol • L^{-1}. The standard curve (D): luminol, 5×10^{-4} mol • L^{-1}; H_2O_2, 0.025 mol • L^{-1}; NaOH, 0.025 mol • L^{-1}.

The analytical performance of aptamer composites

Under the optimal experimental conditions (c(NaOH) = 0.025 mol • L^{-1}, c(H_2O_2) = 0.025 mol •L^{-1}, c(luminol) = 5×10^{-4} mol •L^{-1}), the linear dependence between the CL intensity and thrombin concentration was shown in Fig. 6(D), and the liner range was 2.5×10^{-10} - 1.0×10^{-9} mol • L^{-1}, the original experimental data is shown in Table 1. The limit of detection of 8.3×10^{-11} mol • L^{-1} can be achieved. A complete analysis, including all procedures were performed with a relative standard deviation of 4.9% (n = 11). The results were compared with traditional methods shown in Table 2 and the

results were satisfied.

Table 1 The original experimental data for the standard curve.

$C_{thrombin}/(10^{-10}$ mol/L)	2.5	4	5	6	7	8	9	10
ΔI	253	307	380	449	508	576	635	665

Table 2 Comparing results with conventional methods.

Methods	Liner range (mol·L^{-1})	Detection limit (mol·L^{-1})
Fluorescence [41]		7×10^{-10}
FCS [42]	5×10^{-9} - 5×10^{-7}	2.6×10^{-9}
EIS [43]	3×10^{-10} - 5×10^{-8}	1×10^{-11}
SPR [44]	1×10^{-10} - 1×10^{-7}	1×10^{-10}
ECL [45]	5×10^{-10} -2.5×10^{-8}	2.1×10^{-10}
This work	2.5×10^{-10} - 1.0×10^{-9}	8.3×10^{-11}

Interferences study

To investigated the selectivity of the CL biosensor for detection of thrombin in biology samples, the interferences of some coexisted substances in the thrombin standard solution (thrombin: 3×10^{-11} mol • L^{-1}) was analyzed under the optimal conditions. The tolerable limits of coexisted species were taken as a relative error not larger than 5%, the results were shown in Fig. 7.

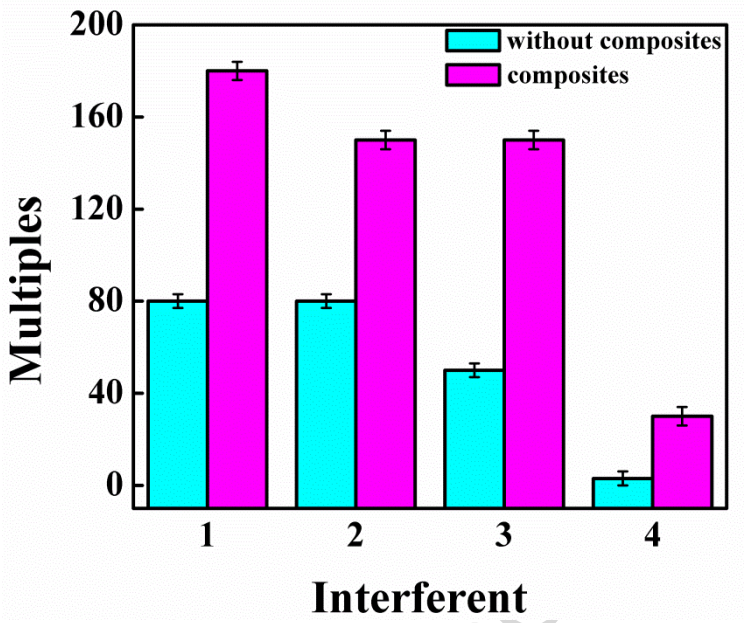

Fig. 7. Interference study of CL sensor that containing composites and without composites.

1. K^+; 2. Bovine Serum Albumin; 3. muramidase; 4. L-cystine.

Application of the CL sensor

In this study, the feasibility of the CL sensor for thrombin detection was investigated. The CL sensor was applied in the detection of thrombin in bovine serum, horse serum and goat serum. As shown in Table 3, the recoveries ranged from 90.32% to 101.0%, under optimal experimental conditions. Apparently, these results were satisfactory, and shown that the CL sensor was of good accuracy and better abilities of anti-interfere. Therefore, the CL sensor was feasible to be used in the detection of thrombin in biology samples.

Table 3 Application of CL sensor.

Samples	Content (mg • L^{-1})	Found (mg • L^{-1})	RSD (%)	Recovery (%)
Bovine serum	10.72	9.66	2.6	90.32
Super horse serum	10.44	9.97	3.2	95.52
Goat serum	10.44	10.54	2.7	101.0

Conclusion

In summary, a CL biosensor was fabricated for quantitative thrombin analysis based on the aptamer composites. Thrombin can be detected with an ultrahigh sensitivity (8.3×10^{-11} mol • L^{-1}), and the sensitivity of this method is higher than other methods [41-45]. Furthermore, the proposed method showed a high specificity to the detection of thrombin in bovine serum, horse serum and goat serum. The obtained CL biosensor was proved to be a better potential method for its biology sample application with high sensitivity and selectivity.

Acknowledgements

This work was supported by the Shandong Provincial Natural Science Foundation of China (No. ZR2016BM01), and Horizontal Scientific Research Project of China (No.W15077).

References

[1] Xuan Weng, Suresh Neethirajan. A microfluidic biosensor using graphene oxide and aptamer-functionalized quantum dots for peanut allergen detection. *Biosensors and Bioelectronics* 85 (2016) 649-656.

[2] Xu Hun, Fang Liu, Zhenhua Mei, Lifeng Ma, Zhouping Wang, Xiliang Luo. Signal amplified strategy based on target-induced strand release coupling cleavage of nicking endonuclease for the ultrasensitive detection of ochratoxin A. *Biosensors and Bioelectronics* 39 (2013) 145-151.

[3] Xu Hun, Yaqiong Xu, Guoliang Xie, Xiliang Luo. Aptamer biosensor for highly sensitive and selective detection of dopamine using ubiquitous personal glucose meters. *Sensor and Actuators B: Chemical* 209 (2015) 596-601.

[4] HongQi Chen, Juan Xu, Fei Yuan, Yong Wu, YiYan Zhang, Lun Wang. A ‘‘turn-off’’ luminescence resonance energy transfer aptamer sensor based on near-infrared upconverting $NaYF_4$:Yb^{3+}, Tm^{3+} nanoparticles as donors and gold nanorods as acceptors. *Chinese Chemical Letters* 24 (2013) 79-81.

[5] Tian-Shyng Ding, Xin-Chun Huang, Yun-Ling Luo, Hsin-Yun Hsu. In vitro investigation of methylene blue-bearing, electrostatically assembled aptamer–silica nanocomposites as potential photodynamic therapeutics. *Colloids and Surfaces B: Biointerfaces* 135 (2015) 217-224.

[6] Yuanyuan Zhuang, Hongping Deng, Yue Su, Lin He, Ruibin Wang, Gangsheng Tong, Dannong He, and Xinyuan Zhu. Aptamer-Functionalized and Backbone Redox-Responsive Hyperbranched Polymer for Targeted Drug Delivery in Cancer Therapy. *Biomacromolecules.*

17 (2016) 2050-2062.

[7] Chun Xia Zhou, Ri Jian Mo, Zhi Meng Chen, Juan Wang, Guo Zhu Shen, Yi Ping Li, Qin Guo Quan, Ying Liu, and Cheng Yong Li. Quantitative Label-Free Listeria Analysis Based On Aptamer Modified Nanoporous Sensor. *ACS Sens.* 1 (2016) 965-969.

[8] Dong Zhu, Rui Xiang Yang, Yu Ping Tang, Wei Li, Zhao Yi Miao, Yue Hu, Jun Chen, Sheng Yu, Juan Wang, Chen Yang Xu. Robust nanoplasmonic substrates for aptamer macroarrays with single-step detection of PDGF-BB. *Biosensors and Bioelectronics* 85 (2016) 429-436.

[9] Yeh-Hsing Lao, Kyle K.L. Phua, and Kam W. Leong. Aptamer Nanomedicine for Cancer Therapeutics: Barriers and Potential for Translation. *ACS Nano.* 9 (2015) 2235-2254.

[10] Dongju Zhang, Juan Han, Yunchao Li, Louzhen Fan, and Xiaohong Li. Aptamer-Based K^+ Sensor: Process of Aptamer Transforming into G‑Quadruplex. *J. Phys. Chem. B* 120 (2016) 6606-6611.

[11] ShaoHua Wu, YiFan Zeng, Liang Chen, You Tang, QiongLin Xu, JianJun Sun. Amplified electrochemical DNA sensor based on hemin/G-quadruplex DNAzyme as electrocatalyst at gold particles modified heated gold disk electrode. *Sensor and Actuators B: Chemical* 225 (2016) 228-232.

[12] ShaoHua Wu, You Tang, Liang Chen, XianGui Ma, SongMao Tian, JianJun Sun. Amplified electrochemical hydrogen peroxide reduction based on hemin/G-quadruplex DNAzyme as electrocatalyst at gold particles modified heated copper disk electrode. *Biosensors and Bioelectronics* 73 (2015) 41-46.

[13] Yit Lung Khung, Dario Narducci. Synergizing nucleic acid aptamers with 1-dimensional nanostructures as label-free field-effect transistor biosensors. *Biosensors and Bioelectronics*

50(2013) 278-293.

[14] Yuezhen He, Jian Sun, Xiaoxun Wang, Lun Wang. Detection of human leptin in serum using chemiluminescence immunosensor: Signal amplification by hemin/G-quadruplex DNAzymes and protein carriers by Fe_3O_4/polydopamine/Au nanocomposites. *Sensor and Actuators B: Chemical* 221 (2015) 792-798.

[15] Gonge Tang, Cailan Zhao, Jie Gao, Hongliang Tan. Colorimetric detection of hydrogen sulfide based on terbium-G-quadruplex-hemin DNAzyme. *Sensor and Actuators B: Chemical* 237 (2016) 795-801.

[16] Danhui Zhang, Xiaoheng Liu and Xin Wang. Green synthesis of graphene oxide sheets decorated by silver nanoprisms and their anti-bacterial properties. *Journal of Inorganic Biochemistry* 105 (2011) 1181-1186.

[17] Ian Y.Y. Bu. Highly conductive and transparent reduced graphene oxide/aluminium doped zinc oxide nanocomposite for the next generation solar cell applications. *Optical Materials* 36 (2013) 299-303.

[18] Mukesh Kumar, Jin Suk Chung, Byung-Seon Kong, Eui Jung Kim, Seung Hyun Hur. Synthesis of graphene–polyurethane nanocomposite using highly functionalized graphene oxide as pseudo-crosslinker. *Materials Letters* 106 (2013) 319-321.

[19] R. Thangappan, S. Kalaiselvam, A. Elayaperumal, R. Jayavel. Synthesis of graphene oxide/vanadium pentoxide composite nanofibers by electrospinning for supercapacitor applications. *Solid State Ionics* 268 (2014) 321-325.

[20] Andrew D. DeYoung, Sang-Won Park, Nilesh R. Dhumal, Youngseon Shim, YounJoon Jung, and Hyung J. Kim. Graphene Oxide Supercapacitors: A Computer Simulation Study. *J. Phys.*

Chem. C 118 (2014) 18472-18480.

[21] Jun Cao, Yongyi Zhang, Chuanling Men, Yanyan Sun, Zhaona Wang, Xuetong Zhang, and Qingwen Li. Programmable Writing of Graphene Oxide/Reduced Graphene Oxide Fibers for Sensible Networks with in Situ Welded Junctions. *ACS Nano.* 8 (2014) 4325-4333

[22] Fei Qu, Dongya Liu, Jinmao You. Fluorescent turn-off/on bioassay for hemoglobin based on dual-emission carbon nanodots-graphene oxide system with multi-detection strategies. *Analytica Chimica Acta* 921 (2016) 59-66.

[23] Zonghua Wang, Jianbo Yu, Rijun Gui, Hui Jin, Yanzhi Xia. Carbon nanomaterials-based electrochemical aptasensors. *Biosensors and Bioelectronics* 79 (2016) 136-149.

[24] Lucas P.H. Saravia, Anandhakumar Sukeri, Josue M. Goncalves, Juan S. Aguirre-Araque, Bruno B.N.S. Brandão, Tiago A. Matias, Marcelo Nakamura, Koiti Araki, Henrique E. Toma, Mauro Bertotti. CoTRP/Graphene oxide composite as efficient electrode material for dissolved oxygen sensors. *Electrochimica Acta* 222 (2016) 1682-1690.

[25] Stefano Borini, Richard White, Di Wei, etc. Ultrafast Graphene Oxide Humidity Sensors. *ACS Nano.*12 (2013) 11166-11173.

[26] Jianmei Yang, Baoting Dou, Ruo Yuan, and Yun Xiang. Proximity Binding and Metal Ion-Dependent DNAzyme Cyclic Amplification-Integrated Aptasensor for Label-Free and Sensitive Electrochemical Detection of Thrombin. *Anal. Chem.* 88 (2016) 8218-8223.

[27] Weiling Song, Qiao Zhang, Xuxu Xie, Shusheng Zhang. Fluorescence aptameric sensor for isothermal circular strand-displacement polymerization amplification detection of adenosine triphosphate. *Biosensors and Bioelectronics* 61 (2014) 51-56.

[28] Pei Zou, Yaling Liu, Hongyong Wang, Jun Wu, Feifan Zhu, Hao Wu. G-quadruplex

DNAzyme-based chemiluminescence biosensing platform based on dual signal amplification for label-free and sensitive detection of protein. *Biosensors and Bioelectronics* 79 (2016) 29-33.

[29] Fenglei Gao, Lili Du, Daoquan Tang, Yao Lu, Yanzhuo Zhang, Lixian Zhang. A cascade signal amplification strategy for surface enhanced Raman spectroscopy detection of thrombin based on DNAzyme assistant DNA recycling and rolling circle amplification. *Biosensors and Bioelectronics* 66 (2015) 423-430.

[30] Jing Zhang, Pingping Chen, XiaoYan Wu, JingHua Chen, LiangJun Xu, GuoNan Chen, FengFu Fu. A signal-on electrochemiluminescence aptamer biosensor for the detection of ultratrace thrombin based on junction-probe. *Biosensors and Bioelectronics* 26 (2011) 2645-2650.

[31] Tao Li, Erkang Wang and Shaojun Dong. Chemiluminescence thrombin aptasensor using high-activity DNAzyme as catalytic label. *Chem. Commun.* 2008, 5520–5522.

[32] Xiaoting Ji, Wei Wang, Xiaoqian Li, Yaoyao Chen, Caifeng Ding. Enhanced chemiluminescence detection of glutathione based on isoluminol-PSM nanoparticles probe. *Talanta* 150 (2016) 666-670.

[33] Rui Liu, Peng Zhang, Huijie Li, Chunsun Zhang. Lab-on-cloth integrated with gravity/capillary flow chemiluminescence (GCF-CL): towards simple, inexpensive, portable, flow system for measuring trivalent chromium in water. *Sensor and Actuators B: Chemical* 236 (2016) 35-43

[34] Feifei Liu, Chunsun Zhang. A novel paper-based microfluidic enhanced chemiluminescence biosensor for facile, reliable and highly-sensitive gene detection of Listeria monocytogenes.

Sensor and Actuators B: Chemical 209 (2015) 399-406.

[35] Zhengbo Chen, Lulu Tan, Liangyu Hu, Yimeng Zhang, Shaoxiong Wang, and Fanyi Lv. Real Colorimetric Thrombin Aptasensor by Masking Surfaces of Catalytically Active Gold Nanoparticles. *ACS Appl. Mater. Interfaces* 8 (2016) 102-108.

[36] W.S. Hummers Jr., R.E. Offeman, Preparation of graphitic oxide. *J. Am. Chem. Soc*. 80 (1958) 1339-1339.

[37] M.Z. Kassaee, E. Motamedi, M. Majdi. Magnetic Fe_3O_4-graphene oxide/polystyrene: fabrication and characterization of a promising nanocomposite. *Chem. Eng. J.* 172 (2011) 540-549.

[38] Basri Gulbakan, Emir Yasun, M. Ibrahim Shukoor, Zhi Zhu, Mingxu You, Xiaohong Tan, Hernan Sanchez, David H. Powell, Hongjie Dai, and Weihong Tan. A Dual Platform for Selective Analyte Enrichment and Ionization in Mass Spectrometry Using Aptamer-Conjugated Graphene Oxide. *J. Am. Chem. Soc*. 132 (2010) 17408-17410.

[39] Prabha Jayapal, Günter Mayer, Alexander Heckel, Frank Wennmohs. Structure–activity relationships of a caged thrombin binding DNA aptamer: Insight gained from molecular dynamics simulation studies. *Journal of Structural Biology*. 166 (2009) 241-250.

[40] Lisa R. PaborskyS, Sarah N. McCurdy, Linda C. Griffin, John J. Toole, Lawrence L. K. Leung. The Single-stranded DNA Aptamer-binding Site of Human Thrombin. *The Journal of Biological Chemistry*, 268 (1993) 20808-20811.

[41] Wei Wang, Dang Dang Xu, Dai Wen Pang, Hong Wu Tang. Fluorescent sensing of thrombin using a magnetic nano-platform with aptamer-target-aptamer sandwich and fluorescent silica nanoprobe. *Journal of Luminescence* 187 (2017) 9-13.

[42] Jinjin Yin, Aidi Zhang, Chaoqing Dong, Jicun Ren. An aptamer-based single particle method for sensitive detection of thrombin using fluorescent quantum dots as labeling probes. *Talanta* 144 (2015) 13-19.

[43] Qingqing Wang, Zhixue Zhou, Yanling Zhai, Lingling Zhang, Wei Hong, Zhiquan Zhang, Shaojun Dong. Label-free aptamer biosensor for thrombin detection based on functionalized graphene nanocomposites. *Talanta* 141 (2015) 247-252.

[44] Hongxia Chen, Fangjie Qi, Hongjian Zhou, Shengsong Jia, Yanmin Gao, Kwangnak Koh, Yongmei Yin. Fe_3O_4@Au nanoparticles as a means of signal enhancement in surface plasmon resonance spectroscopy for thrombin detection. *Sensors and Actuators B: Chemical* 212 (2015) 505-511.

[45] Bangrong Zhuo, Yuqin Li, Xiang Huang, Yuejuan Lin, Yaowen Chen, Wenhua Gao. An electrochemiluminescence aptasensing platform based on ferrocene-graphene nanosheets for simple and rapid detection of thrombin. *Sensors and Actuators B: Chemical* 208 (2015) 518-524.

Graphical abstract

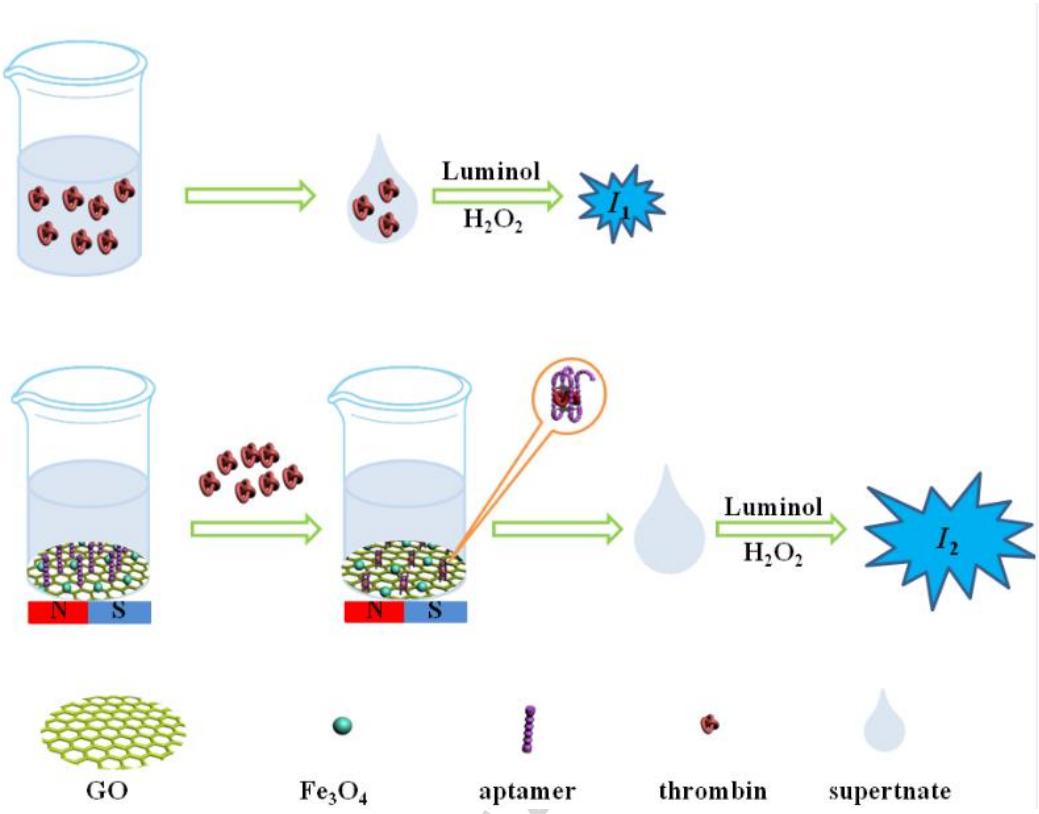

Highlights

1. The aptamer composites were synthesized using graphene oxide (GO) as the backing material.
2. The coupling of luminol CL detection with aptamer composites can significantly increase both the sensitivity and selectivity of the thrombin detection.
3. The aptamer composites could prove useful in sensitive biosensing applications.